



UNIVERSITÀ DI PARMA

ARCHIVIO DELLA RICERCA

University of Parma Research Repository

Development of a convenient ex vivo model for the study of the transcorneal permeation of drugs: histological and permeability evaluation

This is the peer reviewed version of the following article:

Original

Development of a convenient ex vivo model for the study of the transcorneal permeation of drugs: histological and permeability evaluation / Pescina, Silvia; Govoni, Paolo; Potenza, Arianna; Padula, Cristina; Santi, Patrizia; Nicoli, Sara. - In: JOURNAL OF PHARMACEUTICAL SCIENCES. - ISSN 0022-3549. - 104:1(2015), pp. 63-71. [10.1002/jps.24231]

Availability:

This version is available at: 11381/2787693 since: 2021-11-26T15:48:33Z

Publisher:

John Wiley and Sons Inc.

Published

DOI:10.1002/jps.24231

Terms of use:

Anyone can freely access the full text of works made available as "Open Access". Works made available

Publisher copyright

note finali coverpage

(Article begins on next page)

12 August 2025

Development of a convenient *ex vivo* model for the study of the trans-corneal permeation of drugs: histological and permeability evaluation

Silvia Pescina^a, Paolo Govoni^b, Arianna Potenza^c, Cristina Padula^c, Patrizia Santi^c, Sara Nicoli^{c*}

^aInterdepartmental Center Biopharmanet-TEC, University of Parma, Parco Area delle Scienze 27/A, 43124, Parma, I

^bDepartment of Biomedical, Biotechnological and Translational Sciences, University of Parma, Via Volturmo 39, 43126 Parma, I

^cDepartment of Pharmacy, University of Parma, Parco Area delle Scienze 27/A, 43124, Parma, I

*Corresponding Author

Sara Nicoli

Department of Pharmacy, University of Parma

Parco Area delle Scienze 27/A

43124 Parma

I

Tel: +390521905065

Fax: +390521905006

e-mail: sara.nicoli@unipr.it

KEYWORDS

In vitro model

Permeability

Drug transport

Epithelial delivery/permeability

Mucosal drug delivery

Trans-corneal

Permeability

Porcine cornea

Ocular delivery

ABSTRACT

In this paper, an *ex vivo* model for the study of the trans-corneal permeation of drugs, based on porcine tissues, was evaluated. The set-up is characterised by ease of realization, absence of O₂ and CO₂ bubbling and low cost; additionally, the large availability of porcine tissue permits a high throughput. Histological images showed the comparability between porcine and human corneas, confirmed the effectiveness of the isolation procedure. A new de-epithelization procedure based on a thermal approach was also set-up to simulate cornea permeability in pathological conditions. The procedure did not affect the integrity of the underlying layers and allowed the characterization of the barrier properties of epithelium and stroma. Six compounds with different physico-chemical properties were tested: fluorescein, atenolol, propranolol, diclofenac, ganciclovir and lidocaine. The model highlighted the barrier function played by epithelium towards the diffusion of hydrophilic compounds and the permselectivity with regard to more lipophilic molecules. In particular, positively charged compounds showed a significantly higher trans-corneal permeability than negatively charged compounds.

The comparability of results with literature data supports the goodness and the robustness of the model, especially taking into account the behaviour of fluorescein, which is generally considered a marker of tissue integrity.

1 Introduction

Several diseases affect the anterior segment of the eye and topical formulations, such as eye-drops, ointments and gels, represent the simplest and most used treatment approach. However, part of the drug applied topically on the ocular surface is lost due to tear turnover, binding to tear proteins, non-corneal absorption through sclera and conjunctiva, and systemic absorption¹. Additionally, the cornea, due to its complex structure, exerts a high resistance towards xenobiotic permeation. All these phenomena preclude the possibility of a consistent trans-corneal permeation: it has been estimated that approximately 7% of lipophilic and 1% of hydrophilic compounds applied topically could reach the aqueous humor². Furthermore, the cornea can also represent the target of different pathological conditions, such as keratitis - that can evolve to ulcer - neovascularisation, keratoconus and cystinosis.

Different models are currently used to study the trans-corneal permeability, both *in vivo* and *in vitro/ex vivo*. *In vivo* models are mainly based on rodents (rabbit, mouse, rat), while *in vitro/ex vivo* models include epithelial cells layer cultures³, reconstructed cornea⁴ or excised cornea; the latter reproduces the complexity of the whole membrane and allows to investigate the transport phenomena. *In vitro* models are characterized by a good control of experimental conditions and are relatively cheap, although they allow to study only a single step in the absorption process.

Porcine eyes are a good model of human eyes⁵, are easily available and the cornea is simple to isolate and adequately large and robust to handle. This model has already been used in the literature, however, it is poorly characterised in terms of histology and experimental set-up.

The aim of the present paper was to develop a simple and robust *ex vivo* model for the trans-corneal permeation of drugs, based on freshly explanted porcine cornea. The model is easy to set-up, cheap and can give results comparable to other methods reported in the literature, but characterized by more complex set-up such as O₂ and CO₂ bubbling, nutrients addition and special diffusion cells. Furthermore, a new method for epithelium removal, based on a thermal approach and never reported before in the literature for the cornea treatment, was identified, in order to obtain a tissue simulating a condition of compromised epithelium. The full-thickness and de-epithelialized model was evaluated by histological analysis and permeation experiments on Franz-type diffusion cell. As model permeants six compounds of different physico-chemical properties with diagnostic or therapeutic rationale were chosen: a dye [fluorescein (FLUO)], two beta-blockers [atenolol

(ATNL) and propranolol (PRPNL)], a NSAID [diclofenac (DICL)], an antiviral [ganciclovir GCV] and a local anesthetic [lidocaine (LIDO)]. Together with the evaluation of the model, also interesting results on the role of the charge of compounds with similar size and lipophilicity on transcorneal permeation are reported.

2 Materials and methods

2.1 Materials

HEPES ((4-(2-hydroxyethyl)-1-piperazineethanesulfonic acid) was purchased from Sigma-Aldrich (St. Louis, USA) as well as atenolol, diclofenac sodium, fluorescein sodium, ganciclovir and propranolol as hydrochloride; lidocaine as hydrochloride was a gift from Lisapharma SpA (Como, I). Buffered solutions used were HEPES buffered saline (HEPES; 5.96 g/l HEPES, 9.0 g/l NaCl pH 7.4 with NaOH 5N) and phosphate buffered saline (PBS; 0.19 g/l KH₂PO₄, 5.98 g/l Na₂HPO₄•12H₂O, 8.8 g/l NaCl pH 7.4 with H₃PO₄). For HPLC analysis, methanol, acetonitrile (both HPLC grade) and distilled water were used. All other chemicals used were of analytical grade.

2.2 Methods

2.2.1 Tissue preparation

Fresh porcine eyes were isolated from Landrace and Large White pigs (age 10-11 months, weight 145-190 kg, both female and male animals), supplied from a local slaughterhouse (Annoni S.p.A., Parma, I). The eyes were kept in PBS at +4°C until use, that occurred within 2 hours from enucleation. Only bulbs with macroscopically intact corneas were employed, while eyes showing opaque corneas were discarded. The full-thickness corneas (consisting of epithelium, stroma and endothelium) were isolated as corneo-scleral button by cutting with a scalpel beyond the limbus. To obtain de-epithelialized cornea samples, the whole bulb was soaked in 60°C deionized water for two minutes (the epithelium becomes completely opaque). Then, the epithelium was carefully peeled off using a spatula and discarded. To avoid tissue damage during the preparation procedure, the corneal tissues were exposed to air only for few minutes altogether; once prepared, all samples, both full-thickness and de-epithelialized, were kept in saline solution until use, that occurred within 30 minutes.

2.2.2 Tissue characterization

Porcine cornea was characterized in terms of thickness and water content. The thickness was measured by means of a digital calliper (0.001 mm resolution; Absolute Digimatic 547-401, Mitutoyo, Milan, I): corneo-scleral buttons were measured at the central and peripheral (limbial) sections. Furthermore, the thickness of each of the five layers constituting the cornea were derived from the histological images.

For the determination of corneal water content, tissue discs of 9 mm diameter were cut, weighted and then dried at room temperature to constant weight in a dessiccator containing calcium chloride. The water content (%) was calculate as follow:

$$\text{water content (\%)} = (w_i - w_f / w_i) * 100 \text{ equation 1}$$

where w_i e w_f are the initial and the final weight, respectively.

For optical microscopy, corneal samples, both full-thickness and de-epithelialized, just isolated or after permeation experiments, were fixed in 10% formaldehyde, then embedded in paraffin and sectioned using a microtome. Staining was carried out using Harris hematoxylin/eosin⁶. Images were taken using an optical microscope Nikon Eclipse 80i, equipped with a camera Nikon Digital Sight DS-2Mv and connected to the control software, NIS Elements F (Nikon Instruments, Calenzano, I).

Furthermore, porcine eyes were weighed and anatomical axis length was measured; aqueous and vitreous volumes were determined by weighting, assuming that density was 1 g/cm³.

2.2.3 Permeation experiments

Permeation experiments were performed in glass Franz-type diffusion cells (area 0.2 cm²). Full-thickness or de-epithelialized tissues were placed on the cell with the endothelial side facing the receiving compartment.

The donor compartment was filled with 300 µl of solution containing the model compound, dissolved in HEPES buffer at different concentrations (ATNL 2 mg/ml, DICL 1 mg/ml, FLUO 1 mg/ml, GCV 1.5 mg/ml, LIDO 2 mg/ml and PRPNL 0.1 mg/ml). The concentrations have been selected based on the data found in the literature in analogous experiments, for ease of comparison with previously published data. In case of DICL and GCV these concentrations also match the therapeutic ones. The receiving phase consisted of 4 ml of HEPES buffer, thermostatted at 37°C and magnetically stirred to avoid

any boundary layer effect. At predetermined times for up to 5 hours, 300 µl of solution were sampled from the endothelial side and immediately replaced by an equal volume of fresh HEPES buffer.

Blank experiments were conducted to exclude the presence of any interference from the tissue; all experiments were carried out at least in triplicate using always different ocular bulbs from different animals.

2.3 Analytical methods

FLUO was analyzed without any preliminary separation by fluorescence (excitation wavelength 485 nm, emission wavelength 535 nm) with multi-label plate reader (Viktor³ 1420, Wallac). The calibration curve was built with standard solutions between 5 and 250 ng/ml.

ATNL, DICL, GCV, LIDO and PRPNL were analyzed using an HPLC apparatus equipped with an isocratic pump (Perkin Elmer series 200), an autosampler (Prostar 410, Varian, Leinì (To), I) and a UV-Vis spectrophotometric detector (Perkin Elmer LC290 or Shimadzu SPD-20ALC) or, as alternative, by HPLC/UV-Vis Flexar. The analyses were performed at room temperature, unless otherwise indicated. All methods were validated for linearity, accuracy (RE%) and precision (RSD%). Chromatographic conditions are described in detail in Table 1.

2.4 Data processing

Data were presented as amount permeated ($\mu\text{g}/\text{cm}^2$) as a function of time (min). The trans-corneal flux across full-thickness and de-epithelialized cornea (J , $\mu\text{g}/\text{cm}^2\text{min}$) were calculated as the slope of the regression line at steady state, while the apparent permeability coefficient of full-thickness and de-epithelialized cornea (P_{app} , cm/s) were calculated at the steady state as:

$$P_{app} = J/C_D \quad \text{equation 2}$$

where C_D ($\mu\text{g}/\text{ml}$) was the concentration of the donor solution. The lag time (min) was determined as the intercept on the x-axis of the regression line at steady state.

To determine the apparent permeability coefficient across the epithelium ($P_{epithelium}$), the resistance approach was used⁷. The resistance to transport (R) can be written as:

$$R_{cornea} = R_{epithelium} + R_{stroma-endothelium} \quad \text{equation 3}$$

Since the resistance (R) is the inverse of permeability, $P_{\text{epithelium}}$ can be simply calculated as:

$$1/P_{\text{cornea}} = 1/P_{\text{epithelium}} + 1/P_{\text{stroma-endothelium}}$$

equation 4

2.5 Statistical analysis

The results were expressed as mean value \pm standard error of the mean (sem). The difference between values was assessed using one-way ANOVA (Kaleidagraph 4.01 software) and considered statistically significant when $p < 0.05$.

3 RESULTS and DISCUSSION

Rabbit is commonly considered the reference animal model for both *in vivo* and *in vitro* ocular experiments, not only for the ease of handling, but also for a substantial comparability to human cornea. Anyway, there are some differences: the thickness of rabbit cornea is lower than human, Bowman's layer is absent - and this could be relevant on the production of experimental lesions -, Descemet's membrane appears thicker than in human eyes⁸. Bovine and porcine ocular tissues are considered a good alternative to rabbit for *in vitro* studies. Particularly, pig eye is considered a suitable model of the human eye with respect to size⁹, vascular anatomy, histology, physiology^{10,11} and mechanical properties¹². Furthermore, pigs being intended for human consumption, porcine ocular bulbs are easy to get from slaughterhouses.

Literature reports several transport conditions of enucleated eyes from the slaughterhouse to the laboratory: by soaking in saline solution $+4^{\circ}\text{C}$ ^{2,13}, Krebs's buffer at $+4^{\circ}\text{C}$ in which oxygen was continuously bubbled¹⁴, BRS-hepes solution saturated with oxygen at $+4^{\circ}\text{C}$ ¹⁵, but also in a simple closed plastic bag to avoid dehydration, at $+4^{\circ}\text{C}$ ¹⁶.

In the present work, porcine eyes were brought to the laboratory in PBS at $+4^{\circ}\text{C}$ and dissected within 2 hours from enucleation.

3.1 Tissue characterization

3.1.1 Ocular bulb

The porcine eyeball used in this study weights 8.01 ± 0.08 g, while the human one is reported to be 7 g¹⁷; anatomical axis are nearly coincident, being respectively 23.17 ± 0.37

mm for the pig and 24 mm for the human¹⁷, as well as comparable are the volume of the aqueous humor (186±17 µl for porcine eye and 199 µl for the human one¹⁸) and the vitreous body (3.53±0.08 ml and 4 ml for porcine and human bulb-eye¹⁹, respectively). In analogy with the human choroid, porcine eye is devoided of *tapetum lucidum*, a reflective layer oriented toward the retina that makes possible the night vision in many vertebrates⁹. However, some differences can be detected: the thickness of the porcine sclera corresponds to 1.25 mm, that is approximately twice the human sclera, which is 0.6 mm²⁰; furthermore, porcine sclera is generally pigmented, due to the presence of melanin, especially in correspondence of the ciliary arteries, while human sclera appears white¹⁷.

3.1.2 Cornea

Some eyeballs showed undamaged and perfectly transparent corneal membrane, while in others the corneas were damaged and opaque and were immediately discarded; the histological sections (Figure 1) confirmed the reliability of the visual inspection for cornea integrity evaluation.

The histological section of intact cornea shows the integrity of epithelium, stroma and endothelium, demonstrating that neither transport conditions, nor the isolation procedures have damaged the tissue (Figure 1b). From the histological section, the thickness of the single layers that constitute the cornea were measured and the experimental data are compared to literature values, of both porcine and human tissues in Table 2.

The thickness of pig epithelium is twice that of humans¹⁷, while the thickness of the endothelium is identical (5 µm), and porcine stroma is 30% thicker than human¹⁷. Bowman layer measured 5 µm (the literature value for pig is 2 µm⁹, but sometimes is reported as uneven and partially dispersed in the collagen²¹ or hardly visible²²) and it is 8-14 µm thick in man¹⁷. Finally, the Descemet's membrane appear to be comparable to human¹⁷.

The total thickness of the tissue was measured using a digital calliper. While human cornea is characterized by a different thickness between the central part (approximately 500 µm) and the limbial part (approximately 710 µm)¹⁷, the porcine corneas did not show any difference as a function of the position (1188±29 µm in the centre and 1140±24 µm at the limbus), in agreement with the literature values of animals of comparable age⁹.

Cornea water content is considered a sensitive parameter to evaluate the integrity of the tissue²³: a loss of integrity of epithelium or endothelium leads to an increase of the normal corneal water content, that in human corresponds to 78%¹⁷. The water content of porcine corneas resulted 80.6±0.4% when epithelium appeared intact (Figure 1b), while it was

85.5±4.4% in the case of damaged epithelium (Figure 1a). These two values are statistically different ($p < 0.01$), with high reproducibility for intact cornea and considerable variability for altered tissue. Porcine corneal hydration reported in literature is lower, i.e. 71.93±0.47%²⁴ and 77.2±0.7%²¹; the forementioned discordance could be due to differences in the measurement approach and/or the age and race of the animals used.

3.2 Epithelium removal by thermal treatment

The literature reports several methods to remove the corneal epithelium from the underlying stroma, based on mechanical (scalpel blade^{25,26} or gill knife²⁷), enzymatic (Dispase II²⁸), physical (excimer laser²⁹) or chemical approaches (EDTA²⁸ or ethanol²⁹). In this work an alternative method based on a thermal approach was set up. The removal of corneal epithelium was carried out by immersion of the whole eyeball in deionized water at 60°C for two minutes. This method, never reported for corneal tissue, was inspired by the approaches currently used for the separation of the epidermis from the dermis in isolated pig skin^{30,31} and for the removal of the epithelium from porcine esophageal mucosa³².

As shown in the histological sections, the procedure proposed allows the complete removal of the epithelium (Figure 2b), without any damage to the underlying Bowman's layer, which appears completely intact as in the full-thickness sample (Figure 2a). The thermal treatment has no effect on the endothelium either (Figures 2c-d); finally, no signs of edema can be detect in the stroma.

3.3 Permeation experiments

In vitro trans-corneal permeation experiments are generally performed using excised cornea from animal of different species such as rabbit^{7,11,23,33} (the most common), pig^{7,11,14} cow^{7,11}, goat^{13,34} and sheep³⁴. As permeation apparatus several glass cells are employed: vertical Franz-type diffusion cell, as such^{35,36} or modified^{2,13,16,34}; modified Ussing chamber³⁷; horizontal perfusion cells^{33,38}, having a convex surface shape to preserve corneal natural curvature^{14,15}; diffusion cell obtained by modifying a 25 ml Erlenmeyer flask³⁹; furthermore, new alternative systems were proposed, like a polycarbonate corneal perfusion chamber which allows the monitoring of endothelial functionality²⁵. Corneal exposed area is very variable, including values from 0.1 to 1.33 cm²^{11,13,16,23,25,35,37-39}.

During permeation experiments, to preserve the integrity of the tissue and to maintain a constant pH, Krebs buffer¹⁴, bicarbonate Ringer's³³, or glutathione bicarbonate Ringer's buffer^{23,38} are used as donor and receiving solution and oxygen¹⁴ or a mixture of 95% O₂

and 5% CO₂ are bubbled in both compartments^{23,33,38}. However, it has been demonstrated that it is possible to maintain the integrity of the porcine cornea without addition of nutrients and/or oxygenation of the solutions^{16,35,36}. This is the reason why, in the present work, corneal samples (always used within 30 minutes from the arrival to the lab) were simply mounted on a Franz-type diffusion cell (exposed area 0.2 cm²), without adding nutrients or oxygen to donor and receptor solutions, made of pH 7.4 HEPES isotonic buffer. The small exposed area limits the possible cornea distortion due to the curvature of the tissue. To verify if this procedure is acceptable, cornea samples were mounted on diffusion cells and, after 2, 3 and 5 hours, the cells were dismantled and the cornea was sectioned and stained.

The result is presented in Figure 3; all epithelial layers remained intact after 2 hours of permeation (Figure 3a); after 3 hours a slight loosening of the superficial epithelial layers became visible (Figure 3b), while at the end of the permeation experiments (5 hours) the detachment of the most apical layers of the epithelium was undeniable (Figure 3c) even if also the slicing procedure can have an impact on tissue integrity. Nevertheless, the basal side of the epithelium remained intact and no signs of edema were detectable in the upper stroma (Figure 3c). Comparable results were previously reported by Camber and collaborators, who studied the effect of a 4 hours perfusion on isolated porcine cornea²¹. From a macroscopic point of view, the tissue showed a progressive visible opacification over time, probably due to the disorganization of the epithelial superficial layers and to the hydration of the stroma in contact with the endothelial side.

Concerning de-epithelialized samples, a faster progressive opacification took place during the 5 hours experiments due to the complete lack of the epithelium that regulate corneal hydration.

In order to evaluate the model, permeation experiments were performed using six well-characterized compounds, having different physico-chemical properties (Table 3). Experiments were performed across full-thickness cornea and across de-epithelialized cornea in order to evaluate the barrier role of the different layers i.e. epithelium, stroma and endothelium. Among these, the epithelium is generally considered the limiting membrane to diffusion especially for hydrophilic molecules, due to the presence of tight junctions (*zonula occludens*) in the most external layers⁴⁰.

Permeation profiles are shown in Figure 4, while the values of permeability coefficient (Equation 2) are reported in Table 3.

Looking at the profiles, it is evident that the presence of the epithelium in the full-thickness cornea reduces the permeation, especially for the more hydrophilic compounds (FLUO, GCV and ATNL), that can diffuse only following the paracellular pathway. This is reflected in the permeability coefficient values (Table 3): permeability across full-thickness cornea is similar to the permeability across the epithelium, suggesting that the latter represents the rate limiting step.

The most hydrophilic compound tested was sodium fluorescein (molecular radius 4.8 \AA ⁷, net charge at pH 7.4 -1.9 ⁴¹), a highly water-soluble dye used in ophthalmology to assess the integrity of the corneal epithelium, since it binds damaged epithelium and stroma, but not intact epithelium⁴². The permeability coefficient found across intact cornea ($0.05 \cdot 10^{-5} \text{ cm/s}$) is in very good agreement with literature data on porcine cornea ($0.08\text{-}0.12 \cdot 10^{-5} \text{ cm/s}$)⁴³. Concerning GCV, no data referred to diffusion across porcine cornea are available, anyway a similar permeability was reported for *ex vivo* diffusion through rabbit cornea ($P=0.38 \cdot 10^{-5} \text{ cm/s}$)⁴⁴. Also in case of ATNL, a substantial difference between intact cornea and de-epithelialized tissue can be observed, however in this case the permeability coefficient through the full-thickness cornea was not determined, because of the low sensitivity of the analytical method. The more lipophilic compounds, PRNL, DICL and LIDO, are characterized by similar lipophilicity, but different charge at pH 7.4. In general, their permeation across the cornea was less sensitive to the presence of the epithelium, if compared with the hydrophilic model permeants, suggesting that the rate limiting layer is the stroma.

The permeability coefficient of DICL ($\log D_{7.4} 1.31$; 99.9% negatively charged), across full-thickness cornea is comparable to the literature data ($2.3 \cdot 10^{-5} \text{ cm/s}$ ¹⁵ and $0.963 \cdot 10^{-5} \text{ cm/s}$ ¹⁶): when compared to the de-epithelialized tissue, there is still a statistical difference. A completely different behaviour is shown by PRPNL ($\log D_{7.4} 1.38$; 99.8% positively charged) for which the presence of the epithelium increased uniquely and slightly the lag time, but did not affect the permeability coefficient. LIDO ($\log D_{7.4} 1.71$, positively charged) behaves very similarly to PRPNL and the permeability coefficient measured is comparable to literature data ($1.11 \cdot 10^{-5} \text{ cm/s}$ porcine cornea *ex vivo*)¹¹.

The different behaviour of DICL vs. PRPNL and LIDO can be explained, in principle, in terms of (i) differences in partition; (ii) differences in hydrogen bond formation or (iii) differences in permeant charge. The first hypothesis, i.e. differences in partitioning, is not

justified by the logD data reported in the literature. The second hypothesis is related to the number of hydrogen bonds that a molecule can form, as suggested by Kidron and colleagues, who found that the permeability of the cornea decreases by increasing hydrogen bonding capacity ⁴⁵. However, this is not the case, since propranol and diclofenac have the same number of total hydrogen bonding groups ⁴⁶, although they present a 10 fold difference in permeability coefficient. Considering the charge of the permeant (hypothesis iii), it is clear that the negative charged molecule (DACL) shows lower permeability coefficient across the full-thickness tissue and across the epithelium compared with the two positively charged molecules (PRPNL and LIDO), despite the similar size and lipophilicity. On the other hand, the cornea has been shown to be permselective to positively charged compounds by Rojanasakul and Robinson⁴⁷, who reported a higher permeability for positively charged molecules compared to the negative ones. The permselectivity of the tissue probably depends on the negative charge of the cornea at physiological pH, as confirmed by the isoelectric point value of 3.2⁴⁷, and is likely located in the epithelium, because the permeability coefficient across the stroma is similar for the three permeants. Another hypothesis can also be made: the combination between positive charge and lipophilicity makes both PRPNL and LIDO membrane-active compounds (i.e. molecules interacting with membrane lipids), even if with different mechanism^{48,49}. Their activity on epithelial cells membrane could contribute to the obtained result.

It is also important to underline that the permeability coefficient found using this very simple experimental set up are in general comparable to that using constant O₂ or O₂/CO₂ (95/5) bubbling ^{11,15} or pre-incubation in 5% CO₂ atmosphere ⁴³, indicating that the epithelium preserved its barrier properties over the length of the experiment and that the water uptake due to endothelium damage does not impact on tissue permeability, thanks to the robust nature of porcine cornea.

The permeability of drugs across bovine and porcine cornea is reported to be between 3 and 9-fold lower than across rabbit cornea ¹¹. Comparison with the permeability of intact human cornea is not easy, due to the extremely limited data that can be found in the literature. We can hypothesize a lower permeability of pig compared to man, mainly on the basis of the higher thickness.

In Figure 5 the comparison between the barrier role of stroma (full squares; measured) and epithelium (open circles; calculated) is presented. It is clear that for hydrophilic compounds (FLUO, ATNL and GCV), permeation is limited by the epithelium, while for

lipophilic molecules (propranolol and lidocaine), the diffusion across the stroma represents the limiting step, mainly for the low partitioning between the lipophilic and the hydrophilic layers ⁴⁰. The barrier role of endothelium, a monolayer with weak junctions (*macula occludens*) that constitute a leaky lipophilic layer, can be neglected ⁵⁰.

Permeability coefficients through de-epithelialized cornea appear comparable for all the molecules tested and independent from lipophilicity and net charge (Table 3). This result has been expected and is ascribed to the structure and high porosity of the corneal stroma, a thick, fibrous and acellular layer, mainly consisting of water (78%) and collagen fibrils (15%), whose permeability depends strongly on molecular radius and only a little on distribution coefficient ⁷. The composition of the stroma strictly recalls the composition of the sclera, the other ocular connective tissue that protect the eye. Due to this similarity, cornea and sclera have been suggested to have similar permeability ³⁹ and the data collected in the present paper confirm this finding. In fact, the permeability coefficients found across the stroma (Table 3) are comparable to that obtained through porcine sclera for LIDO ($P=1.66 \cdot 10^{-5}$ cm/s ¹¹) and PRPNL ($P=0.60 \cdot 10^{-5}$ cm/s ⁵¹) and through bovine sclera for FLUO and ATNL ($P=0.52 \cdot 10^{-5}$ cm/s ⁵² and $P=0.89 \cdot 10^{-5}$ cm/s ⁵³, respectively).

4 Conclusions

In this paper, an *ex vivo* model for the study of the trans-corneal permeation of drugs, based on porcine tissues, was evaluated. The set-up is characterised by ease of realization, absence of O₂ and CO₂ bubbling and low cost; additionally, the large tissue availability permits a high throughput, in particular if compared with *ex vivo* studies carried out using corneas from euthanized animals (generally rabbits). The comparability of the present data with permeability data reported in the literature using complex set-up such as O₂ and CO₂ bubbling, nutrients addition and special diffusion cells, supports the goodness and the robustness of the model, especially taking into account the behaviour of fluorescein, which is generally considered a marker of tissue integrity. Additionally, thanks to the thermal de-epithelization procedure, reported here for the first time for the corneal tissue, it is possible to collect useful information on the barrier properties of the different layers and to simulate cornea permeability in pathological conditions, where the epithelium is absent or compromised. This is for instance the case of keratitis and ulcers, but also of corneal neovascularization. In this paper, the possible role of active transport systems present in corneal epithelium as well as drug accumulation inside the different corneal

layers have not been considered and further studies will be necessary to assess the usefulness of this model to this regard.

The data collected has also highlighted the role of the charge on the transcorneal permeability of molecules with similar size and lipophilicity.

Aknowledgements

The financial support of Italian Ministry of Education, University and Research (PRIN2010H834LS) is gratefully acknowledged.

Tables

Table 1. HPLC experimental conditions

Condition Drug	Column	λ (nm)	Flow (ml/min)	Aqueous phase	Organic phase	Volume ratio (a:o)	LLOQ ^a ($\mu\text{g/ml}$)
Atenolol	Nova-pak C18 4 μm 3.9 x 150 mm (Waters)	226	0.6	1.57 g/l sodium 1- heptanesulfonate 1.01 g/l Na_2HPO_4 2.9 ml/l dibutylamine adjusted to pH 3 with 85% H_3PO_4	Methanol	70:30	5
Diclofenac	Nova-pak C18 4 μm 3.9 x 150 mm (Waters)	284	1	5.98 g/l Na_2HPO_4 0.19 g/l KH_2PO_4 adjusted to pH 7.4 with 85% H_3PO_4 Addition of 5 mM triethylamine	Acetonitrile	60:40	1
Ganciclovir	Jupiter C18 5 μm 4.6 x 150 mm (Phenomenex) ^b	254	1.2	Water	-	-	0.5
Lidocaine	Nova-pak C18 4 μm 3.9 x 150 mm (Waters)	230	1	2.4 g/l NaH_2PO_4 adjusted to pH 8 with 85% H_3PO_4	Methanol	25:75	1
Propranolol	Bondclone C18 10 μm 3.9 x 300 mm (Phenomenex)	225	1.2	0.2% v/v H_3PO_4	Acetonitrile	70:30	0.25
^a Lower Limit of Quantification							
^b Thermostatted at 30°C							

Table 2. Thickness of the different corneal layer of human and porcine cornea

	Porcine		Human
	Experimental data ^a	Literature data	Literature data ¹⁷
Epithelium	105 μm	47 μm ⁵⁴ 55.7 μm ²¹	50 μm
Bowman's layer	5 μm	2 μm ⁹	8-14 μm
Stroma	750 μm	700 μm ⁹	500 μm
Descemet's membrane	11 μm	8-12 μm ⁹ 12-15 ²¹	5-15 ^b μm
Endothelium	5 μm	4.5 μm ⁵⁴	5 μm

^aMeasured from histological sections
^bThickening from 5 to 15 μm during lifetime

Table 3. Physico-chemical properties and permeability coefficients of the compounds tested.

Drug	MW (Da)	pK _a s	LogD _{7.4}	P _{full-thickness} ^a *10 ⁻⁵ (cm/s)	P _{stroma-endothelium} ^a *10 ⁻⁵ (cm/s)	P _{epithelium} ^b *10 ⁻⁵ (cm/s)
FLUO	332.31	6.4	-4.28 ⁷	0.05±0.02	1.52±0.10	0.05±0.01
GCV	255.23	2.2, 9.4	-2.10 ⁵⁵	0.23±0.06	1.65±0.06	0.27±0.01
ATNL	266.34	9.32	-1.5 ⁵⁶	nd ^c	1.59±0.24	not calculable
DICL	296.15	4.0	1.31 ⁵⁷	0.53±0.02	1.78±0.13	0.75±0.02
PRPN	259.34	9.23	1.38 ⁵⁷	1.46±0.05	1.73±0.04	9.40±1.06
LIDO	234.34	7.96	1.71 ⁵⁷	1.18±0.07	1.54±0.03	5.08±0.31

^aExperimental data, calculated from equation 2
^bCalculated data from equation 4
^cNot determined, due to the high LLOQ of the analytical method (Table 1)

Figures

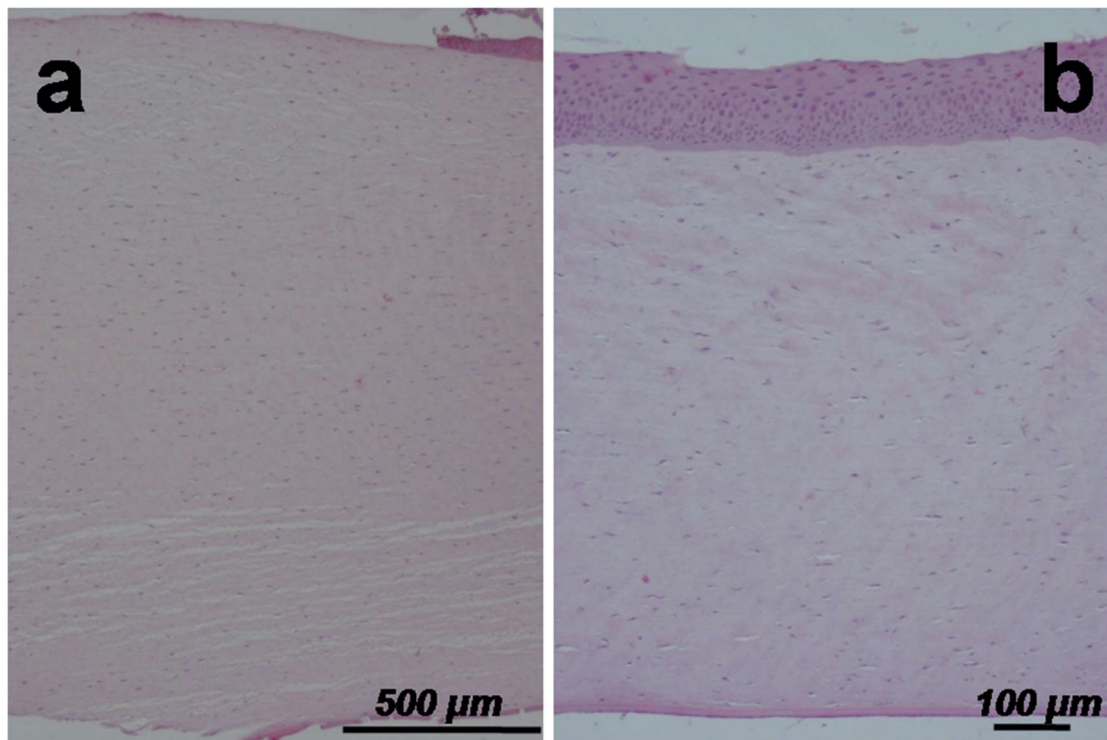


Figure 1. Histological section of opaque and transparent corneas, as estimated by macroscopic evidence. Panel a) Opaque cornea: the image shows the breakage of the corneal epithelium, with exposure of the underlying Bowman's layer, which is followed by water diffusion associated to an uncontrolled hydration (particularly evident the edematous condition in the portion next to the Descemet's membrane) that leads to increase stromal thickness and, consequently, causes the rupture of the endothelium. Panel b) Transparent cornea: the histology shows the integrity of epithelium, stroma and endothelium.

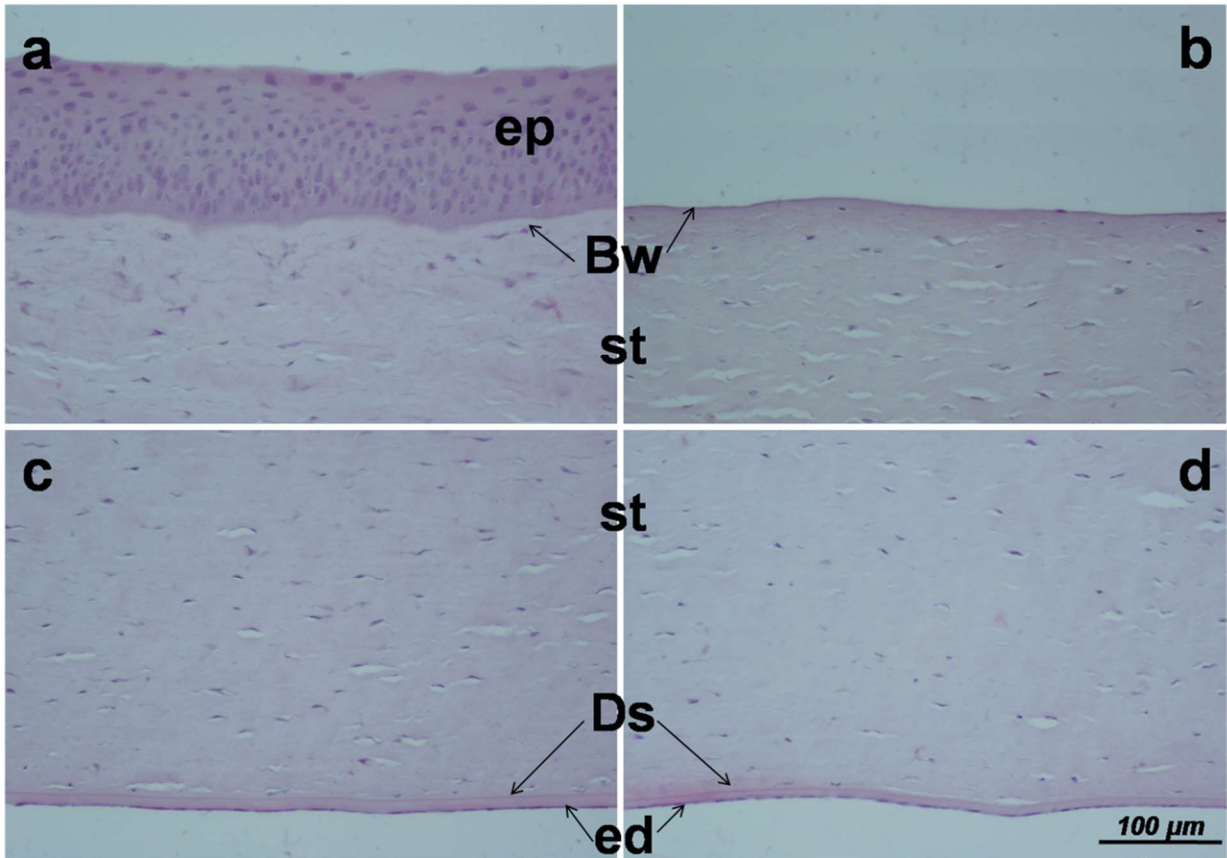


Figure 2. Histological sections of full-thickness (a-c) and de-epithelialized (b-d) porcine cornea. (ep: epithelium; Bw: Bowman's layer; st: stroma; Ds: Descemet's membrane; ed: endothelium; scale bar 100 μ m)

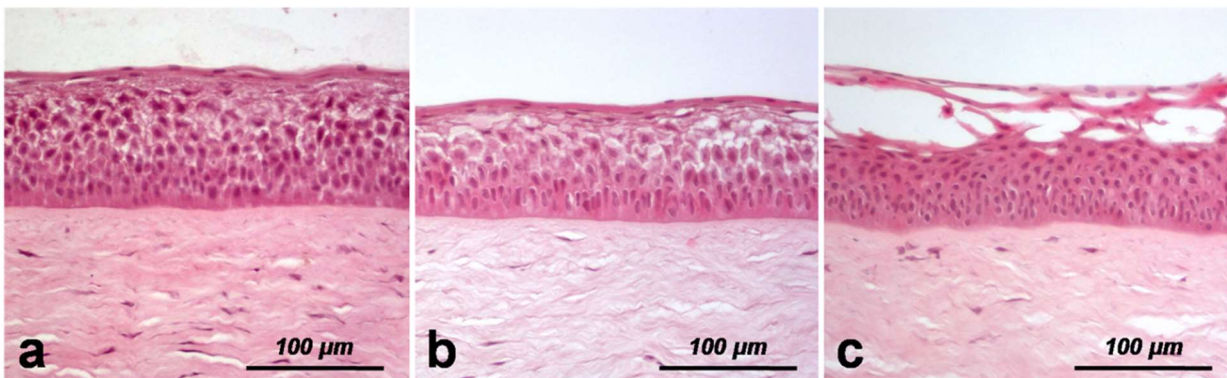


Figure 3. Histological sections of full-thickness cornea after 2 (a), 3 (b) and 5 (c) hours of permeation experiments.

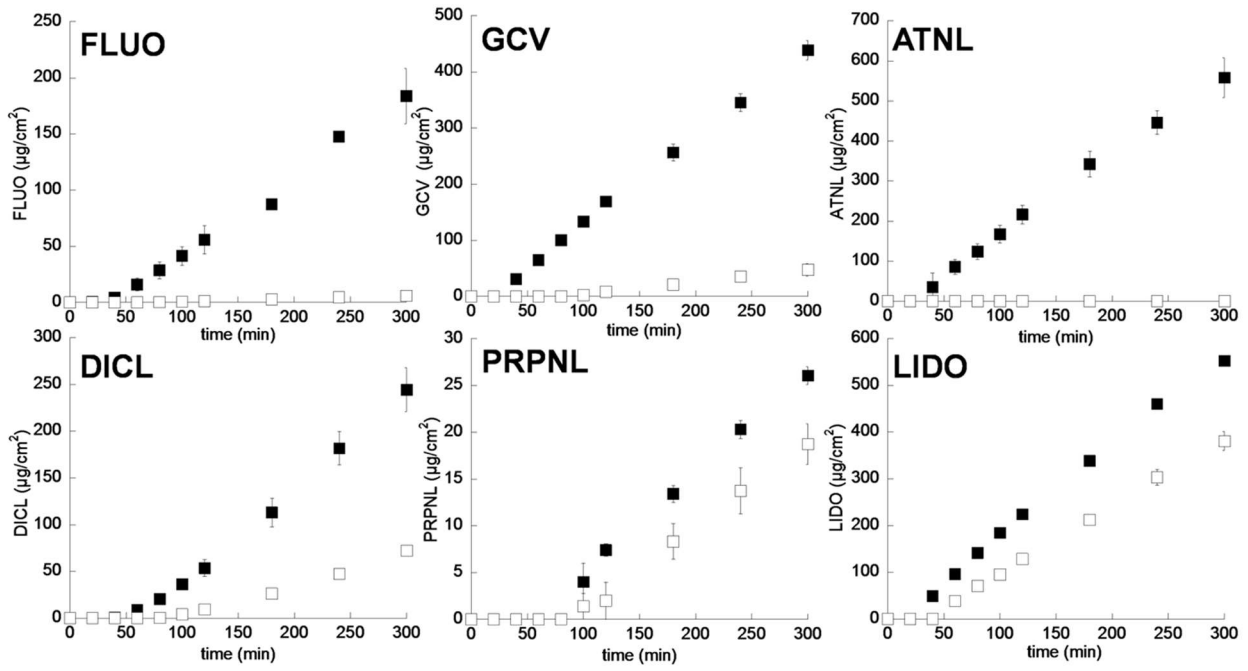


Figure 4. Permeation profiles of model permeants across de-epithelialized (full square) and full-thickness (open square) tissues

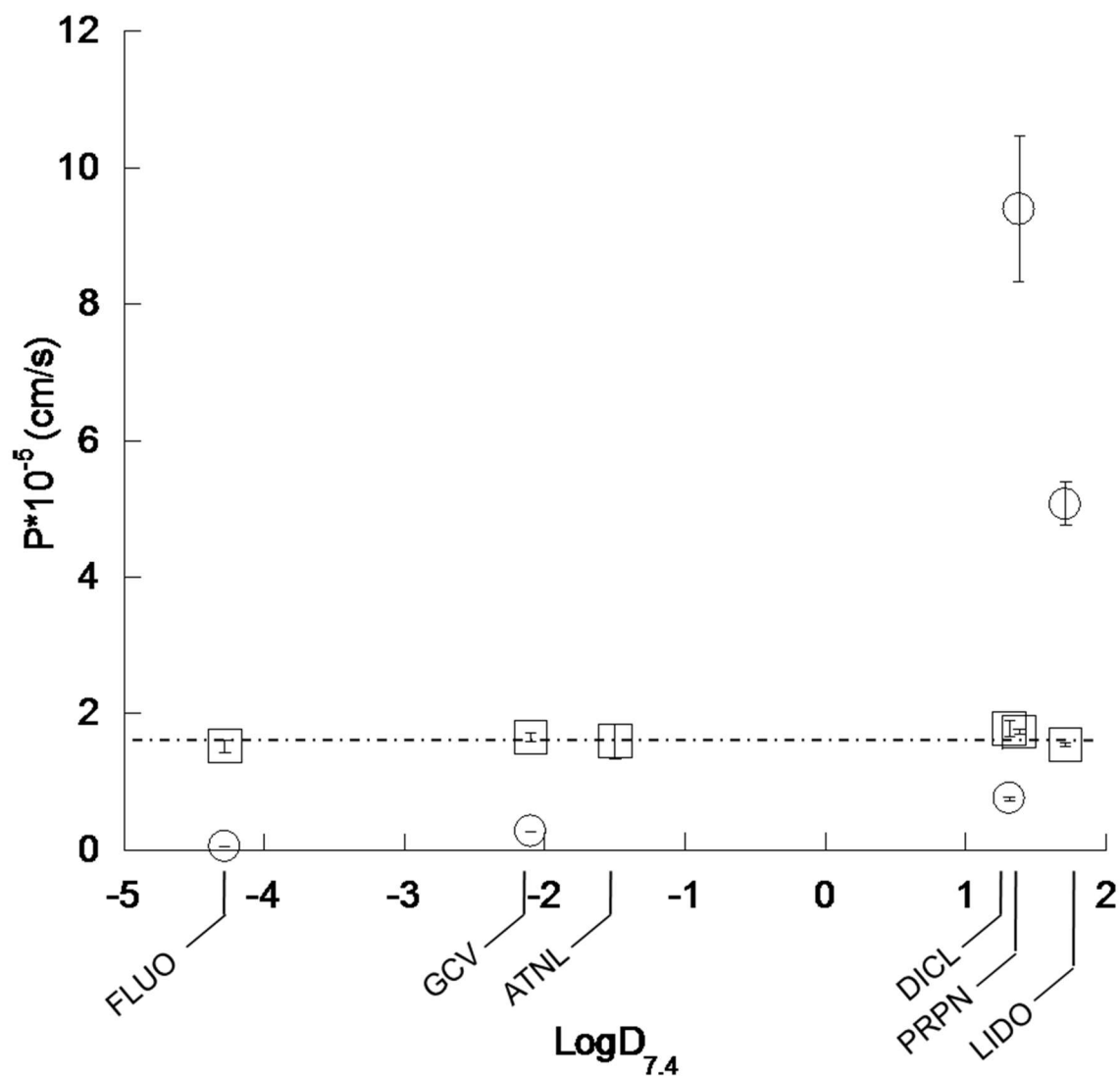


Figure 5. Permeability coefficients of tested compounds across porcine corneal epithelium (open circles; calculated) and de-epithelialized cornea (open squares; measured) as function of $\text{LogD}_{7.4}$ (data from Table 3). $P_{\text{stroma-endothelium}}$ from experimental data (Equation 2); $P_{\text{epithelium}}$ calculated from Equation 4. The $P_{\text{epithelium}}$ for atenolol is not present, since it was impossible to calculate the permeability coefficient across full-thickness cornea. Diclofenac and propranolol have very similar $\text{LogD}_{7.4}$ but very different permeability across the epithelium, being propranolol ten fold more permeable.

REFERENCES

1. Lee VHL. 2003. *Ophthalmic Drug Delivery Systems*. ed.: Dekker.
2. Chandran S, Roy A, Saha RN 2008. Effect of pH and formulation variables on in vitro transcorneal permeability of flurbiprofen: a technical note. *AAPS PharmSciTech* 9:1031-1037.
3. Reichl S 2008. Cell culture models of the human cornea - a comparative evaluation of their usefulness to determine ocular drug absorption in-vitro. *J Pharm Pharmacol* 60:299-307.
4. Reichl S, Bednarz J, Muller-Goymann CC 2004. Human corneal equivalent as cell culture model for in vitro drug permeation studies. *Br J Ophthalmol* 88:560-565.
5. Van den Berghe C, Guillet MC, Compan D 2005. Performance of porcine corneal opacity and permeability assay to predict eye irritation for water-soluble cosmetic ingredients. *Toxicology in Vitro* 19:823-830.
6. Bancroft JD. 1975. *Histochemical techniques*. ed., London, UK: Butterworths.
7. Prausnitz MR, Noonan JS 1998. Permeability of cornea, sclera, and conjunctiva: a literature analysis for drug delivery to the eye. *Journal of Pharmaceutical Sciences* 87:1479-1488.
8. Davies FA 1929. *The Anatomy and Histology of the Eye and Orbit of the Rabbit*. *Trans Am Ophthalmol Soc* 27:400-441.
9. Prince JH, Diesem CD, Eglitis I, Ruskell GL. 1960. *Anatomy and histology of the eye and orbit in domestic animals*. ed., Springfield Illinois USA: Charles C. Thomas.
10. Kivell TL, Doyle SK, Madden RH, Mitchell TL, Sims EL 2009. An interactive method for teaching anatomy of the human eye for medical students in ophthalmology clinical rotations. *Anatomical Sciences Education* 2:173-178.
11. Loch C, Zakelj S, Kristl A, Nagel S, Guthoff R, Weitschies W, Seidlitz A 2012. Determination of permeability coefficients of ophthalmic drugs through different layers of porcine, rabbit and bovine eyes. *Eur J Pharm Sci* 47:131-138.
12. Kling S, Remon L, Perez-Escudero A, Merayo-Llodes J, Marcos S 2010. Corneal biomechanical changes after collagen cross-linking from porcine eye inflation experiments. *Investigative ophthalmology & visual science* 51:3961-3968.
13. Ahuja M, Dhake AS, Majumdar DK 2006. Effect of formulation factors on in-vitro permeation of diclofenac from experimental and marketed aqueous eye drops through excised goat cornea. *Yakugaku Zasshi* 126:1369-1375.
14. Gokce EH, Sandri G, Bonferoni MC, Rossi S, Ferrari F, Guneri T, Caramella C 2008. Cyclosporine A loaded SLNs: evaluation of cellular uptake and corneal cytotoxicity. *Int J Pharm* 364:76-86.
15. Reer O, Bock TK, Müller BW 1994. In vitro corneal permeability of diclofenac sodium in formulations containing cyclodextrins compared to the commercial product voltaren ophtha. *Journal of Pharmaceutical Sciences* 83:1345-1349.
16. Baydoun L, Muller-Goymann CC 2003. Influence of n-octenylsuccinate starch on in vitro permeation of sodium diclofenac across excised porcine cornea in comparison to Voltaren ophtha. *Eur J Pharm Biopharm* 56:73-79.
17. Remington LA. 2012. *Clinical anatomy and physiology of the visual system*. Third ed., St. Louis: Elsevier.
18. Fontana ST, Brubaker RF 1980. Volume and depth of the anterior chamber in the normal aging human eye. *Archives of Ophthalmology* 98:1803-1808.
19. Shroff A. 2011. *An Eye on Numbers: A Ready Reckoner in Ophthalmology*. ed., Kurla, India: Post Script Media PVT. Ltd.
20. Nicoli S, Ferrari G, Quarta M, Macaluso C, Govoni P, Dallatana D, Santi P 2009. Porcine sclera as a model of human sclera for in vitro transport experiments: histology, SEM, and comparative permeability. *Molecular vision* 15:259-266.

21. Camber O, Rehbinder C, Nikkila T, Edman P 1987. Morphology of the pig cornea in normal conditions and after incubation in a perfusion apparatus. *Acta Vet Scand* 28:127-134.
22. Svaldeniene E, Babrauskiene V, Paunksniene M 2003. Structural features of the cornea: light and electron microscopy. *Vet Med Zoot* 46:50-55.
23. Monti D, Saccomani L, Chetoni P, Burgalassi S, Saettone MF 2003. Effect of iontophoresis on transcorneal permeation 'in vitro' of two beta-blocking agents, and on corneal hydration. *Int J Pharm* 250:423-429.
24. Xu YG, Xu YS, Huang C, Feng Y, Li Y, Wang W 2008. Development of a rabbit corneal equivalent using an acellular corneal matrix of a porcine substrate. *Molecular vision* 14:2180-2189.
25. Thiel MA, Morlet N, Schulz D, Edelhauser HF, Dart JK, Coster DJ, Williams KA 2001. A simple corneal perfusion chamber for drug penetration and toxicity studies. *The British Journal of Ophthalmology* 85:450-453.
26. Huang HS, Schoenwald RD, Lach JL 1983. Corneal penetration behavior of beta-blocking agents II: Assessment of barrier contributions. *Journal of Pharmaceutical Sciences* 72:1272-1279.
27. O'Brien WJ, Edelhauser HF 1977. The corneal penetration of trifluorothymidine, adenine arabinoside, and idoxuridine: a comparative study. *Investigative ophthalmology & visual science* 16:1093-1103.
28. Spurr SJ, Gipson IK 1985. Isolation of corneal epithelium with Dispase II or EDTA. Effects on the basement membrane zone. *Invest Ophthalmol Vis Sci* 26:818-827.
29. Kanitkar KD, Camp J, Humble H, Shen DJ, Wang MX 2000. Pain after epithelial removal by ethanol-assisted mechanical versus transepithelial excimer laser debridement. *J Refract Surg* 16:519-522.
30. Hedberg CL, Wertz PW, Downing DT 1988. The time course of lipid biosynthesis in pig epidermis. *J Invest Dermatol* 91:169-174.
31. Law S, Wertz PW, Swartzendruber DC, Squier CA 1995. Regional variation in content, composition and organization of porcine epithelial barrier lipids revealed by thin-layer chromatography and transmission electron microscopy. *Arch Oral Biol* 40:1085-1091.
32. Diaz Del Consuelo I, Pizzolato GP, Falson F, Guy RH, Jacques Y 2005. Evaluation of pig esophageal mucosa as a permeability barrier model for buccal tissue. *J Pharm Sci* 94:2777-2788.
33. Schoenwald RD, Huang HS 1983. Corneal penetration behavior of beta-blocking agents I: Physicochemical factors. *Journal of Pharmaceutical Sciences* 72:1266-1272.
34. Mohanty B, Mishra SK, Majumdar DK 2013. Effect of formulation factors on in vitro transcorneal permeation of voriconazole from aqueous drops. *J Adv Pharm Technol Res* 4:210-216.
35. Vaka SR, Sammeta SM, Day LB, Murthy SN 2008. Transcorneal iontophoresis for delivery of ciprofloxacin hydrochloride. *Curr Eye Res* 33:661-667.
36. Gratieri T, Gelfuso GM, Thomazini JA, Lopez RFV 2010. Excised porcine cornea integrity evaluation in an in vitro model of iontophoretic ocular research. *Ophthalmic Research* 43:208-216.
37. Fuchsjaeger-Mayrl G, Zehetmayer M, Plass H, Turnheim K 2002. Alkalinization increases penetration of lidocaine across the human cornea. *J Cataract Refract Surg* 28:692-696.
38. Camber O 1985. An in vitro model for determination of drug permeability through the cornea. *Acta Pharm Suec* 22:335-342.
39. Ahmed I, Gokhale RD, Shah MV, Patton TF 1987. Physicochemical determinants of drug diffusion across the conjunctiva, sclera, and cornea. *J Pharm Sci* 76:583-586.
40. Järvinen K, Järvinen T, Urtti A 1995. Ocular absorption following topical delivery. *Adv Drug Deliver Rev* 16:3-19.

41. Zanetti-Domingues LC, Tynan CJ, Rolfe DJ, Clarke DT, Martin-Fernandez M 2013. Hydrophobic fluorescent probes introduce artifacts into single molecule tracking experiments due to non-specific binding. *PLoS One* 8:e74200.
42. Morgan PB, Maldonado-Codina C 2009. Corneal staining: do we really understand what we are seeing? *Cont Lens Anterior Eye* 32:48-54.
43. Stewart JM, Schultz DS, Lee OT, Trinidad ML 2009. Collagen cross-links reduce corneal permeability. *Invest Ophthalmol Vis Sci* 50:1606-1612.
44. Tirucheraï GS, Dias C, Mitra AK 2002. Corneal permeation of ganciclovir: mechanism of ganciclovir permeation enhancement by acyl ester prodrug design. *Journal of ocular pharmacology and therapeutics : the official journal of the Association for Ocular Pharmacology and Therapeutics* 18:535-548.
45. Kidron H, Vellonen KS, del Amo EM, Tissari A, Urtti A 2010. Prediction of the corneal permeability of drug-like compounds. *Pharm Res* 27:1398-1407.
46. National Center for Biotechnology Information PubChem Compound Database (accessed Mar. 29, 2014).
47. Rojanasakul Y, Robinson JR 1989. Transport mechanisms of the cornea: characterization of barrier permselectivity. *International Journal of Pharmaceutics* 55:237-246.
48. Hogberg CJ, Lyubartsev AP 2008. Effect of local anesthetic lidocaine on electrostatic properties of a lipid bilayer. *Biophys J* 94:525-531.
49. Först G, Cwiklik L, Jurkiewicz P, Schubert R, Hof M 2014. Interactions of beta-blockers with model lipid membranes: Molecular view of the interaction of acebutolol, oxprenolol, and propranolol with phosphatidylcholine vesicles by time-dependent fluorescence shift and molecular dynamics simulations. *Eur J Pharm Biopharm* 87:559-569.
50. Bucolo C, Drago F, Salomone S 2012. Ocular drug delivery: a clue from nanotechnology. *Front Pharmacol* 3:188.
51. Pescina S, Santi P, Ferrari G, Padula C, Cavallini P, Govoni P, Nicoli S 2012. Ex vivo models to evaluate the role of ocular melanin in trans-scleral drug delivery. *European Journal of Pharmaceutical Sciences* 46:475-483.
52. Cheruvu NPS, Escobar ER, Kompella UB 2005. Transscleral Transport: Barrier Properties of Sclera, Choroid-Tapetum, and Retinal Pigment Epithelium. *Invest Ophthalmol Vis Sci* 46:5390-.
53. Cheruvu NPS, Kompella UB 2006. Bovine and porcine transscleral solute transport: influence of lipophilicity and the Choroid-Bruch's layer. *Investigative ophthalmology & visual science* 47:4513-4522.
54. Merindano MD, Costa J, Canals M, Potau JM, Ruano D 2002. A comparative study of Bowman's layer in some mammals: Relationships with other constituent corneal structures. *Eur J Anat* 6:133-139.
55. Ganellin CR, Triggle DJ. 1997. *Dictionary of Pharmacological agents*. ed., London: Chapman & Hall.
56. Rosenbaum SE. 2011. *Basic Pharmacokinetics and Pharmacodynamics: An Integrated Textbook and Computer Simulations* ed., Hoboken, New Jersey: John Wiley & Sons.
57. Avdeef A, Box KJ, Comer JE, Hibbert C, Tam KY 1998. pH-metric logP 10. Determination of liposomal membrane-water partition coefficients of ionizable drugs. *Pharm Res* 15:209-215.